Displacement Chromatography of Amino Acids: Effects of Selectivity Reversal

Giorgio Carta and Adam A. Dinerman
Center for Bioprocess Development, Dept. of Chemical Engineering, University of Virginia, Charlottesville, VA 22903

Separating mixtures of α-amino butyric acid (ABA) and isoleucine (Ile) by displacement chromatography with a cation exchange resin and an alkaline displacer leads to the formation of a displacement train, in which only ABA is recovered as a pure component, while Ile is recovered in a mixed band with ABA. The purity of the Ile band depends on the concentration of the displacer, and essentially pure Ile is obtained when the displacer concentration is reduced to a low value. The observed behavior is explained by considering the nonideality of the equilibrium uptake of these amino acids by the resin. An equilibrium model, representing the pure component isotherms, predicts variable selectivity and the occurrence of selectivity reversal in the two-component system. Analyses using this model based on the theory of coherent waves and a numerical solution of the conservation equations for the displacement chromatography process agree with the observed behavior, predicting the formation of "azeotropic" bands during the development of the displacement train. Such analyses are used to determine under what conditions a complete separation may be obtained for a given experimental system.

Introduction

Displacement development is one of the fundamental modes of operation of chromatography originally recognized by Tiselius. The technique, intrinsically a nonlinear chromatographic process, exploits the competitive adsorption of components on a highly saturated adsorbent surface.

The rudiments of displacement chromatography have been recognized since the early 1900s in the pioneering work of Tswett. The classical theoretical analyses by Tiselius, Glueckauf (1949), Helfferich and Klein (1970), and Rhee and Amundson (1982) have provided firm bases for understanding these processes. However, the main focus of such theoretical treatments has typically been on systems that can be represented by the competitive Langmuir adsorption model. Practical systems that can be represented, at least approximately, in this fashion are common. On the other hand, such a representation can lead to serious errors when significant deviations from the ideal Langmuirian behavior are present.

A consequence of the competitive Langmuir isotherm, when used in its correct, thermodynamically consistent form (Kemball et al., 1948), is that the selectivity between any pair of components is constant, independent of concentration. For such a system, it is predicted that, when a strong displacer is used, a displacement train with the components fully separated and arranged in order of increasing affinity for the sorbent is formed in a sufficiently long column. However, this is not generally true for systems that exhibit significant variations of the selectivity as a function of concentration. Basmadjian et al. (1987), for example, have pointed out a number of experimental adsorption systems in which both gaseous and liquid phase solutes are adsorbed following non-Langmuir behavior. In some extreme cases a reversal of the selectivity as a function of concentration was observed, resulting in the formation of "azeotropic" mixtures in frontal chromatography experiments. An "extended Langmuir isotherm" was used to explain the results in a semiquantitative manner. A large departure from ideal Langmuirian behavior has also been observed by Paludetto et al. (1987) for the adsorption of chloroaromatic mixtures on zeolites. These authors found that it was necessary to take into account the nonideality of the adsorbed phase in order to make reliable predictions of the breakthrough behavior for mixtures of these compounds.

Recently, Antia and Horvath (1991) have provided an analysis of isotachic patterns in displacement chromatography tak-

Correspondence concerning this article should be addressed to G. Carta.

ing into account selectivity reversal effects. Their analysis was based on the separation of a mixture of two components, A and B, whose adsorption equilibrium is represented by the relationships $q_A = q_A(C_A, C_B)$ and $q_B = q_B(C_A, C_B)$. The mixture is separated by displacement chromatography with a displacer D, of concentration C_D, having an affinity for the sorbent greater than that of either of the feed mixture components. For these conditions, the development of concentration bands in the column, downstream of the displacer front, is governed by the binary adsorption equilibria of A and B. Following Antia and Horvath, a condition necessary for the establishment of fully resolved bands in this process is expressed as:

$$\lim_{C_A \to 0} \left[\frac{q_A(C_A, C_B^*)}{C_A} \right] < \frac{q_D}{C_D} \tag{1a}$$

$$\lim_{C_B \to 0} \left[\frac{q_B(C_A^*, C_B}{C_B} \right] > \frac{q_D}{C_D} \tag{1b}$$

where q_D is the adsorbent loading with D at its concentration C_D. In these inequalities, C_A^* and C_B^* are respectively the concentrations that components A and B would attain in an isotachic displacement train in which the two species are fully resolved in pure component bands. The values of C_A^* and C_B^* depend only on the pure component adsorption equilibria and the displacer concentration. Thus, they are calculated from the well-known Glueckauf relationship (Glueckauf, 1949):

$$\frac{q_A(C_A^*, 0)}{C_A^*} = \frac{q_B(0, C_B^*)}{C_B^*} = \frac{q_D}{C_D} \tag{2}$$

Using competitive adsorption isotherms generated with the ideal adsorbed solution theory (Myers and Prausnitz, 1965) and Eq. 2, Antia and Horvath showed that the stability condition 1 leads to the definition of regions in the $C_A - C_B$ plane (the "hodograph" plane) where a complete separation is possible; a complete separation is possible, but the components are eluted in reverse order; and a complete separation is not possible. The key concept in this analysis is that whether a complete separation is possible or not is determined by the competitive multicomponent behavior rather than purely by the single component isotherms, as would be predicted by the Glueckauf condition. Experimental evidence of the behavior predicted by these conditions has been reported by Subramanian and Cramer (1989) and Cramer (1993) for the chromatography of biological macromolecules. In such systems, the adsorbed molecules can be quite different in size, and significant deviations from Langmuirian behavior can be expected to be quite severe in multicomponent systems. Further work on non-Langmuir equilibrium effects on displacement chromatography separations has been reported by de Bokx et al. (1992). No selectivity reversal was found by these authors, but it was shown that an accurate prediction of band profiles could only be obtained by taking into account nonidealities in the adsorbent.

The objective of this article is to present an analysis of the selectivity reversal effects that we have found for the separation of mixtures of the two amino acids α-amino butyric acid (ABA) and isoleucine (Ile). The displacement chromatography of mixtures of these two compounds with a cation exchange resin resulted in an incomplete separation, the origins of which can be explained in terms of the nonideal equilibrium uptake behavior of these species. A semiempirical model taking into account the heterogeneity of the ion-exchange resin is used to fit binary exchange data and predict multicomponent uptake. This model predicts variable selectivity and selectivity reversal to occur for certain conditions. We show that, although the manner in which the selectivity varies is different from that assumed by Antia and Horvath in their analysis of isotachic patterns, their stability criterion is consistent with the observed formation of "azeotropic" mixtures of ABA and Ile in our experiments. For these conditions, we use the theory of coherent waves to predict the band profiles under local equilibrium conditions and then compare the experimental results with a numerical solution of the conservation equations for the displacement chromatography process. The study extends the prior knowledge of selectivity reversal effects to the ion exchange of these relatively small molecules and sets forth a simple approach for the analysis of the results.

Separation of Amino Acids by Ion Exchange

Ion exchange is frequently used for the recovery and separation of amino acids, both in analysis and in industrial applications. These molecules are amphoteric and may be positively or negatively charged depending upon the solution pH. Thus, these compounds are readily taken up by a cation exchange resin at a solution pH below the isoelectric point, and then efficiently released at a pH above the pI (Yu et al., 1987; Carta et al., 1988).

The separation of mixtures of amino acids by displacement chromatography may be effectively carried out with these resins. The amino acid mixture is first loaded on a column of resin in the hydrogen form at a low pH, and then eluted with an alkaline solution containing, for example, NaOH. A traveling high-pH front is obtained. Upstream of this front the resin is converted to the sodium form and is devoid of amino acids. Downstream, the amino acids become concentrated by the displacement effect and separated as a result of differences in the specific affinities of the amino acid cations for the resin and by virtue of differences in their ionization constants. This type of displacement separations of amino acids in unbuffered solutions was pioneered by Partridge and coworkers (for example, Partridge and Brimley, 1951) over 40 years ago, and is used in industry for process applications. In recent years, a number of authors (Yu et al., 1987; Carta et al., 1988; Gosling et al., 1989; Saunders et al., 1989) have reexamined these separations with an emphasis on modeling and optimization.

Experimental Section

The resin used in this study, Dowex 50W-X8 (Dow Chemical Company, Midland, MI), is a gel-type, sulfonated, styrene-divinylbenzene copolymer with a nominal degree of cross-linking of 8%. A single lot of commerical resin was sieved to recover a fraction with a wet particle size in the range 50–60 μm. The relevant properties of this resin have been reported by Dye et al. (1990). The resin was pretreated with repeated washes with HCl and NaOH solutions and thoroughly rinsed with distilled-deionized water as described in that article. The sulfonated gel-type resin Dowex 50W-X4 was also used for some of the experiments. This resin is similar in structure to

Dowex 50W-X8, but it has a lower nominal degree of cross-linking of 4%. A 400 mesh sample of this resin, pretreated as described above, was used. This resin was found to have essentially the same ion-exchange capacity as Dowex 50W-X8 on a dry-weight basis. The two resins, thus, differ essentially only in the extent of hydration as a result of the different degree of cross-linking.

Amino acids in L and D,L form were obtained from Sigma Chemical Co. (St. Louis, M0) and Ajinomoto USA, Inc. (Raleigh, NC). Other chemicals were obtained from Sigma and Fisher. Analyses of solutions containing amino acids were performed by HPLC with the method described by Dye et al.

Uptake equilibria were obtained by allowing samples of hydrated resin in the hydrogen form to come to equilibrium with a solution containing various initial concentrations of an amino acid. The experiments were done in a constant temperature bath at 25 ± 1°C and the amino acid uptake was calculated as described by Dye et al.

Displacement chromatography experiments were performed with a laboratory scale apparatus. The resin samples were slurry-packed in 1.5-cm-ID glass chromatographic columns with nominal lengths of 20 and 40 cm (Spectrum Scientific). Packed-bed heights of 18 and 36 cm were obtained for the resin in the hydrogen form. The resin beds appeared to shrink by less than 10% when the resin was changed to the sodium form. Laboratory metering pumps (FMI, Mod. RP-SY) were used to supply feed, displacer, regenerant and rinse solutions to the column. The column effluent was followed with a flow-through pH monitor (Pharmacia-LKB, Mod. 2195) and by collecting fractions with a fraction collector (Gilson, Mod. 201) for later analyses by HPLC. No attempt was made to obtain an exact calibration of the pH monitor since this proved unreliable. The pH monitor was thus used simply to determine in a qualitative manner the occurrence of breakthrough of NaOH. Prior to an experiment, the resin was regenerated with 1 N NaOH, converted to the hydrogen form with 1 N HCl, and rinsed with distilled-deionized water. Mixtures of the two amino acids in distilled-deionized water were then loaded onto the column with a metering pump at superficial velocity of 3 cm/min. The displacer consisted of solutions of NaOH in water and was supplied to the column immediately following application of the feed mixture at the same velocity of 3 cm/min. As shown by DeCarli et al. (1990), this results in a very effective ion displacement separation for different mixtures of amino acids in relatively short columns.

Results and Discussion

Uptake equilibria

The equilibrium uptake of α-amino butyric acid by the hydrogen form of the resin is shown in Figure 1. The data were obtained for solutions containing different HCl concentrations. The uptake of amino acid by the resin, q_A, is expressed on a dry weight basis, as a function of the total concentration of amino acid in solution. As shown by Saunders et al. (1989), for a given value of C_A, the uptake of amino acid by the resin increases as the chloride concentration is reduced, approaching a maximum as the chloride concentration approaches zero. For these conditions, the solution pH approaches the pI of the amino acid, and competition from hydrogen ion for the resin's functional groups is minimized. Similar results were obtained

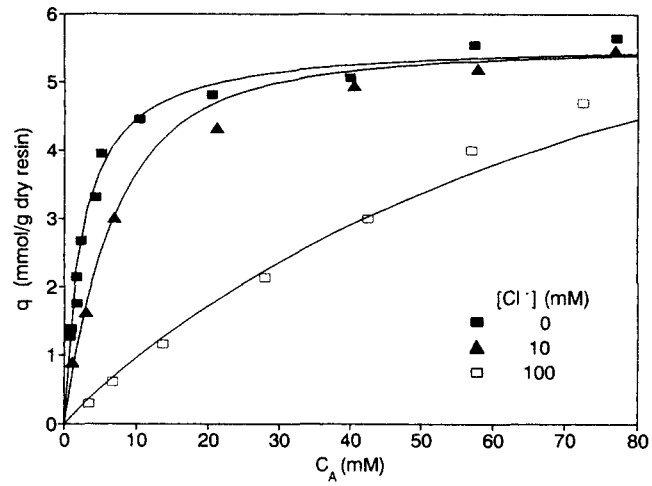

Figure 1. Equilibrium uptake of ABA from hydrochloric acid solutions by Dowex 50W-X8.
Lines are model calculations.

for the uptake of isoleucine by the resin and are given by Dye et al. (1990).

The uptake of amino acids by cation exchange resins is known to occur largely via the stoichiometric exchange of amino acid cations (Yu et al., 1987; Saunders et al., 1989). Therefore, it is dependent solely on the ionic fraction of amino acid cations in solution. This quantity can be calculated by relating the concentrations of amino acid cations, anions and zwitterions to the total concentration $C_A = C_{A^+} + C_{A^\pm} + C_{A^-}$ through the dissociation equilibria and using the electroneutrality condition. The following equations are obtained (Saunders et al., 1989):

$$C_{A^+} = \frac{C_A}{1 + K_1/C_{H^+} + K_1K_2/C_{H^+}^2} \tag{3}$$

$$C_{A^-} = \frac{C_A}{1 + C_{H^+}/K_2 + C_{H^+}^2/K_1K_2} \tag{4}$$

$$C_{A^+} + C_{H^+} = C_{A^-} + K_W/C_{H^+} + C_{Cl^-} \tag{5}$$

where K_1 and K_2 are the dissociation constants of the amino acid and K_W is the ionic product of water. These equations can be solved to compute the solution pH from known values of C_A and C_{Cl^-}. Once the pH is known, the ionic fraction of amino acid cations is given by:

$$X_A = \frac{C_{A^+}}{C_{A^+} + C_{H^+}} \tag{6}$$

Finally, the selectivity coefficient for the exchange of amino acid cations and hydrogen ion can be calculated as:

$$S_{A,H} = \frac{Y_A}{Y_H}\frac{X_H}{X_A} = \frac{Y_A}{1 - Y_A}\frac{1 - X_A}{X_A} \tag{7}$$

where $Y_A = q_A/q_0$. The results of these calculations performed for the αABA uptake data of Figure 1 are shown in Figure

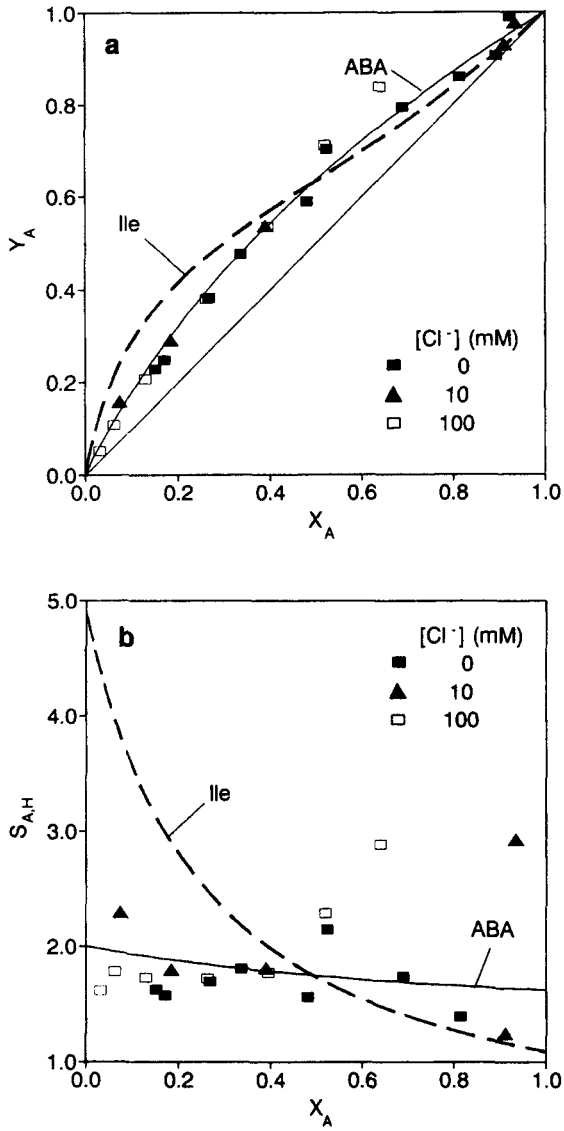

Figure 2. Reduced equilibrium uptake by Dowex 50W-X8 in terms of ionic fractions (a), and selectivity coefficient for the exchange of amino acid cations and hydrogen ion (b).

Dashed lines are correlated values for Ile from Dye et al. (1990).

2a. For a comparison the correlated results for isoleucine obtained by Dye et al. (1990) are also given in these figures. These calculations indicate that the uptake of both amino acids can indeed be assumed to be the result of the stoichiometric exchange of ions. In fact, the amino acid uptake is the same, independent of pH and co-ion concentration, so long as the ionic fraction X_A is the same. Moreover, these results show that the apparent selectivity coefficient relative to hydrogen ion, $S_{A,H}$, varies considerably with resin loading. For both species, the selectivity coefficient decreases with resin loading, but the decrease is much more pronounced for isoleucine than for ABA. Figure 2b shows both the experimental and the correlated selectivity coefficient for ABA and the correlated selectivity coefficient values for isoleucine. Much greater scatter is evident in this plot as the experimental errors are amplified when the selectivity coefficient is calculated from the Y and X values.

Variable apparent selectivity coefficients in ion exchange of both inorganic and organic ions have been reported by several authors, as discussed for example, by Helfferich (1962). Jones and Carta (1993) have recently investigated systematically the effects of molecular size, hydrophobicity and resin cross-linking on the ion-exchange behavior of amino acids. Generally, greater variations in the selectivity coefficient with loading were seen with more highly cross-linked resins and with larger molecular species. In extreme cases, with large dipeptides, only a partial loading of the resin could be obtained. At low loadings, on the other hand, it was found that more hydrophobic amino acids and dipeptides were more strongly retained, irrespective of the molecular size and degree of cross-linking. An explanation was advanced that the apparent variations of $S_{A,H}$ is the result of local heterogeneities associated with the uneven distribution of cross-links in the microstructure of the resins. At low resin loadings, ion exchange occurs on the most selective accessible functional groups. In this limit, the selectivity coefficient is determined by the hydrophobic character of the amino acid. At higher loadings, however, ion exchange occurs on functional groups which are in less accessible sites. Steric hindrance becomes important for these conditions and the result is a decrease in the apparent selectivity coefficient.

When the observed uptake behavior of the two amino acids ABA and isoleucine is compared, the trends described above are also seen. At low loadings, the resin shows a greater preference for the more hydrophobic species, isoleucine. At higher loadings, however, the preference is for the smaller species, ABA. In order to describe this equilibrium behavior quantitatively we have adopted a model based on the assumption that the resin contains a heterogeneous distribution of functional groups (Myers and Byington, 1986; Saunders et al., 1989). The overall uptake behavior is determined by the contribution of each individual group. Therefore, it is possible to describe the behavior of systems with variable selectivity coefficients. In its simplest formulation, the model assumes that the resin comprises only two types of functional groups: one with low selectivity and one with high selectivity. The overall selectivity for ion i relative to a common reference counterion j, in a system containing N counterions is given by (Dye et al., 1990):

$$S_{i,j}=\bar{S}_{i,j}\frac{\sum_{k=1}^{N}\bar{S}_{k,j}(W_{k,j}/W_{i,j}+W_{i,j}/W_{k,j})X_k}{\sum_{k=1}^{N}\bar{S}_{k,j}(1/W_{k,j}+W_{k,j})X_k} \tag{8}$$

The uptake of each component is given by:

$$Y_i=\frac{q_i}{q_0}=\frac{S_{i,j}X_i}{\sum_{k=1}^{N}S_{i,j}X_k} \tag{9}$$

As shown by Myers and Byington, although this expression is based on a simple two-site, binomial distribution, the results are found to be essentially the same that would be obtained

virtually with any distribution having the same average selectivity, the same variance, and the same skewness.

For each $N-1$ binary there are two parameters: an average selectivity coefficient, $\bar{S}_{i,j}$, and a heterogeneity parameter, $W_{i,j}$. The latter parameter is a function of the heterogeneity of the resin's functional groups for the exchange of ions i and j. When $W_{i,j}$ is unity for all the binaries, the apparent selectivity coefficients are constant, independent of ionic composition. The model parameters for ABA and Ile were determined from a least-square fit of the experimental data for each binary exchange system. The resulting values are given in Table 1 and curves calculated with these values are shown in Figures 1 and 2. The $S^0_{i,H}$ values given in this table are the apparent selectivity coefficients at infinite dilution obtained for $X, Y \to 0$.

Selectivity reversal-azeotropic behavior

The term azeotropic behavior is used here in a manner similar to Basmadjian et al. (1987) to indicate fluid-solid equilibria which, at a given temperature and total solute concentration, exhibit one (or more) states characterized by identical mole (or ionic) fractions of the solutes in the two phases. For certain values of the parameters $\bar{S}_{i,j}$ and $W_{i,j}$, Eq. 8 describes such an azeotropic behavior. In the system of two amino acids with a cation exchange resin considered here, the separation occurs in the absence of counterions other than the amino acid cations and hydrogen ion. Since the pK-values of the two species are estimated to be the same, the degree of ionization of the two are also identical. In this case, the ionic fractions of the amino acid cations and total concentrations of the two species are in the same ratio. Moreover, for these conditions, the separation factor $\alpha_{B,A} = q_B C_A / q_A C_B$ coincides with the selectivity coefficient for the exchange of the two amino acids cations, $S_{B,A} = S_{B,H}/S_{A,H}$. Thus, for a given concentration of the co-ion, the equilibrium behavior and the relative selectivity of the two species may be represented simply in terms of their total concentrations.

Calculated uptake curves for the two pure components at $C_{Cl^-} = 0$ and the corresponding "hodograph" plane for mixtures of the two components are given in Figures 3a and 3b, respectively. ABA and isoleucine are identified as A and B respectively. Figure 3a shows that the single-component uptake curves cross at a concentration of approximately 5 mM. The hodograph plane, on the other hand, obtained from the multicomponent uptake isotherm, shows a region where the selectivity coefficient (and the separation factor) is greater than unity and one where it is smaller than unity. The two regions are separated by a unit selectivity line that emerges from the y-axis at a value $C_B \sim 24$ mM. This behavior is different, for example, from that predicted by the ideal adsorbed solution theory (IAS) with Langmuirian single component isotherms. This theory would predict that all points of unit selectivity between two components, if they exist at all, are connected by a straight line with a slope -1 on the hodograph plane (Antia and Horvath, 1991). The observed behavior is also somewhat different to several examples of azeotropic behavior reported by Basmadjian et al. (1987). Multicomponent equilibria in these systems were expressed with an "extended Langmuir isotherm," which predicted unit selectivity lines emerging from the origin of the hodograph plane.

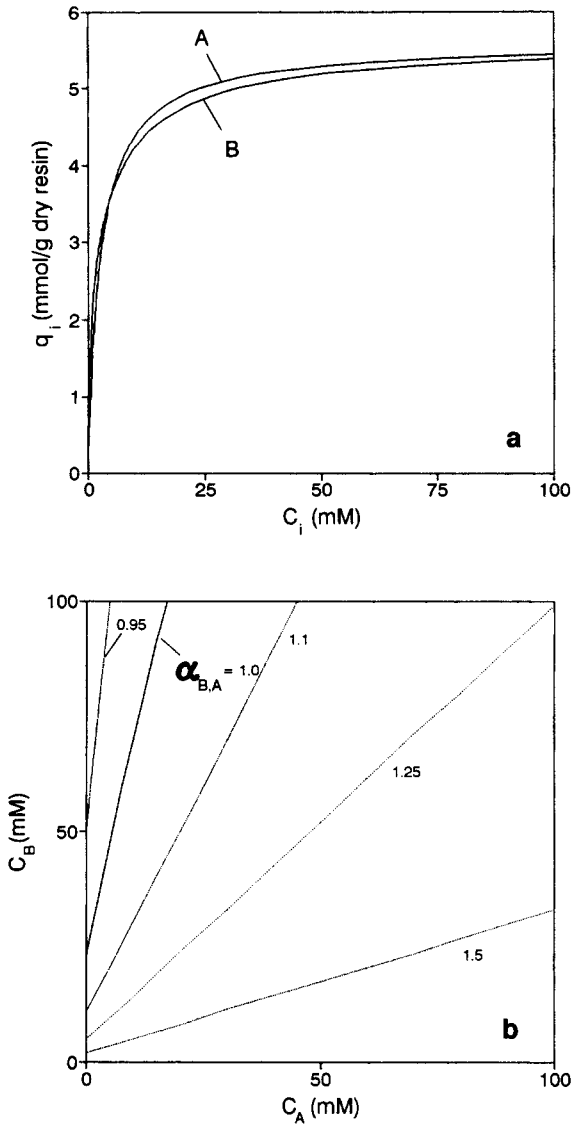

Figure 3. Equilibrium uptake of ABA (A) and Ile (B) by Dowex 50W-X8.

(a) Pure component uptake; (b) hodograph plane showing lines of constant selectivity for the uptake of binary mixtures.

Table 1. Equilibrium Uptake Parameters

	pK_1	pK_2	$\bar{S}_{i,H}$	$W_{i,H}$	$S^0_{i,H}$
ABA	2.36*	9.68*	1.80	1.64	2.02
Ile	2.36**	9.68**	2.31†	4.00†	4.91

*Estimated.
**Meister (1965).
†Dye et al. (1990).

Displacement chromatography dynamics

To describe the dynamic behavior of displacement chromatography separations, we use the classical theory of coherent waves introduced by Glueckauf (1949) and summarized by Ruthven (1984). Neglecting axial dispersion the conservation equation for each feed component is given by:

$$\epsilon \frac{\partial C_i}{\partial t} + \rho_b \frac{\partial q_i}{\partial t} + \epsilon v \frac{\partial C_i}{\partial z} = 0 \tag{10}$$

where ϵ is the void fraction, ρ_b is the bed density, and v is the fluid velocity. With the assumption of local equilibrium and negligible axial dispersion (that is, for "ideal" chromatography), the characteristic velocity for a given composition (C_A, C_B) is given for each component by:

$$v_i = \frac{v}{1 + \frac{\rho_b}{\epsilon}\left(\frac{dq_i}{dC_i}\right)_{C_A, C_B}} \tag{11}$$

for a simple wave, and by:

$$v_i^s = \frac{v}{1 + \frac{\rho_b}{\epsilon}\frac{\Delta q_i}{\Delta C_i}} \tag{12}$$

for a shock. In Eq. 11, dq_i/dC_i is the directional derivative given by:

$$\frac{dq_i}{dC_i} = \frac{\partial q_i}{\partial C_i} + \frac{\partial q_i}{\partial C_j}\frac{dC_j}{dC_i} \tag{13}$$

where the partial derivatives calculated from the uptake equilibrium isotherm. The ratio $\Delta q_i/\Delta C_i$ in Eq. 12 for a shock front is also calculated using the uptake isotherm from the expression:

$$\frac{\Delta q_i}{\Delta C_i} = \frac{q_i(C_A', C_B') - q_i(C_A'', C_B'')}{C_i' - C_i''} \tag{14}$$

where $'$ and $''$ refer to conditions upstream and downstream of the shock front, respectively.

The establishment of coherent waves requires that $v_i = v_j$, yielding for simple waves:

$$\frac{\partial q_i}{\partial C_j}\left(\frac{dC_j}{dC_i}\right)^2 + \left(\frac{\partial q_i}{\partial C_i} - \frac{\partial q_j}{\partial C_j}\right)\frac{dC_j}{dC_i} - \frac{\partial q_j}{\partial C_i} = 0 \tag{15}$$

For each pair of concentrations in the hodograph plane we can compute the coefficients of this quadratic equation from the multicomponent isotherm expression and solve it to find the slopes dC_j/dC_i of the coherent paths followed by simple waves. Similarly, for shock waves, $v_i^s = v_j^s$, which yields:

$$\frac{q_i(C_A', C_B') - q_i(C_A'', C_B'')}{C_i' - C_i''} = \frac{q_j(C_A', C_B') - q_j(C_A'', C_B'')}{C_j' - C_j''} \tag{16}$$

As for simple waves, the shock path in the hodograph can be generated by substituting the multicomponent equilibrium relations in this expression. Rules allowing one to decide whether simple or shock waves are obtained are summarized by Ruthven (1984).

The dynamics of evolution of concentration profiles for a binary displacement separation can be followed completely on the hodograph plane provided that the displacer is more strongly retained by the sorbent than any of the feed component for any concentration level. In this case, no ternary mixtures are formed and the characteristics are contained in the hodograph plane shown in Figure 4 for the ABA/Ile separation. In the example considered in this figure, the feed mixture is represented by point e and consists of an equimolar mixture of the two components (25 mM each). The NaOH displacer concentration is assumed to be 100 mM and is represented by point a on the Ile axis.

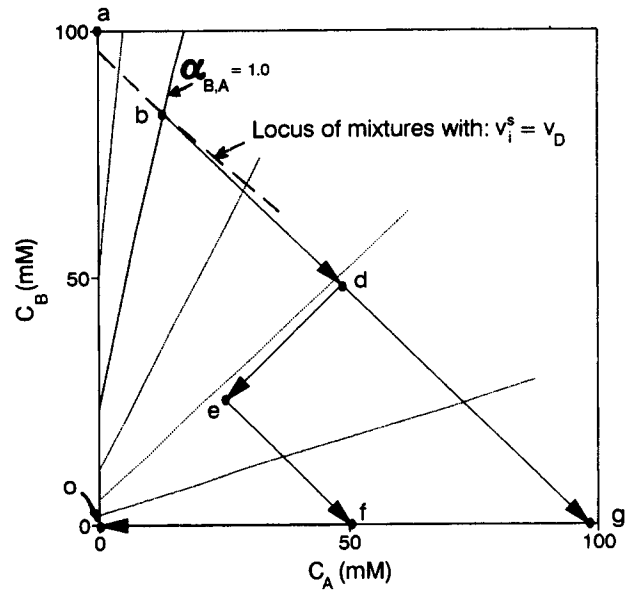

Figure 4. Hodograph plane showing characteristics for the separation of an equimolar mixture of ABA (A) and Ile (B) with 100 mM NaOH.

The corresponding isotachic concentrations of the two components that would be obtained from the Glueckauf condition (Eq. 2) if a complete separation were possible are $C_A^* = 97.3$ and $C_B^* = 96.1$ mM. It is easily verified from the multicomponent equilibrium expressions, that for these conditions, Eq. 1a is not satisfied while Eq. 1b is; that is, the condition necessary to obtain a pure band of the trailing component B is invalid as the unit separation line would have to be crossed to accomplish this state. A partial separation is obtained instead for these conditions. The course of this partial separation can be followed on the hodograph plane and in Figure 5 which gives the column band profiles at different times. Shocks are obtained during the initial loading phase of the displacement chromatography process and the coherent path *efo* is followed. During this phase, the profile within the column will contain a pure band of ABA, about 50 mM in concentration, followed by the feed mixture. After the feed loading phase ($t = 100$ min), supply of the displacer is started with $C_D = 100$ mM. Since NaOH is taken up essentially irreversibly by the resin, the NaOH front moves at a velocity:

$$v_D = \frac{v}{1 + \frac{\rho_b}{\epsilon}\frac{q_D}{C_D}} = \frac{v}{1 + \frac{\rho_b}{\epsilon}\frac{q_0}{C_D}} \tag{17}$$

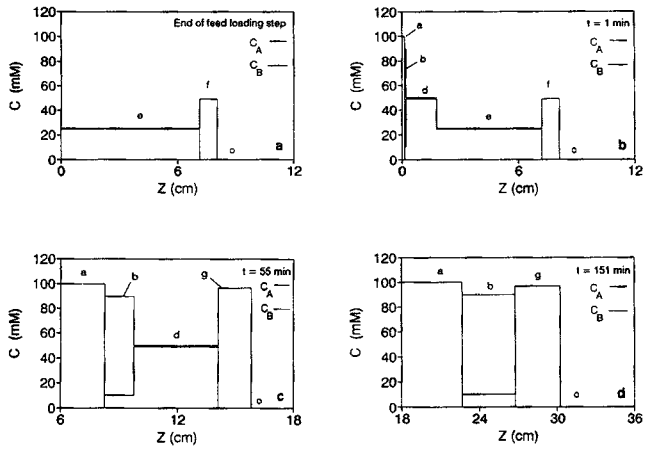

Figure 5. Column band profiles during development of displacement train under ideal conditions.

b, d, e, f and g correspond to states in the hodograph plane; a corresponds to pure NaOH.

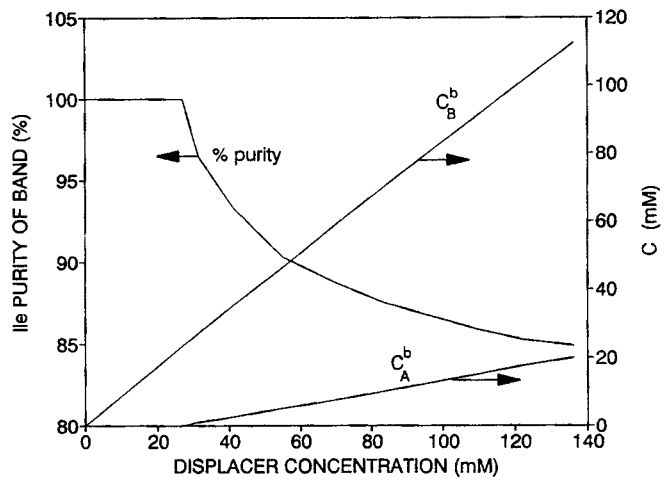

Figure 6. Predicted composition of azeotropic bands formed during the development of the displacement train and purity of the Ile band as a function of the displacer NaOH concentration.

where q_0 is the resin capacity. A coherent azeotropic mixture is obtained downstream of this front. The composition of this mixture is found at the intersection, b, of the unit selectivity line with the locus of points for which the characteristic shock velocity is equal to the displacer velocity. For this mixture the condition:

$$\frac{q_A(C_A^b, C_B^b)}{C_A^b} = \frac{q_B(C_A^b, C_B^b)}{C_B^b} = \frac{q_D}{C_D} \tag{18}$$

is satisfied. Point b is a stable state. In fact, starting at this point, if the C_A were perturbed towards larger values, $\alpha_{B,A}$ $(= S_{B,A})$ would acquire values greater than unity, which would result in an increase in C_B. Such a decrease in C_B, in turn, would tend to reduce $\alpha_{B,A}$ back to the original value of 1. A similar effect would be found if C_B were perturbed towards smaller values. C_A would tend to increase at the rear boundary of the displacement train, restoring an $\alpha_{B,A}$-value of one.

The concentration profile in the bed follows the path *bdefo* with each point corresponding to a plateau. The e-plateau is unstable since its rear boundary moves faster than its front boundary and disappears quickly. The profile then follows the *bdgo* path. Again, the d-plateau is unstable and shrinks until it too disappears giving rise to the path *bgo*. This is an isotachic train along which all waves have the same velocity. From this point on the profile retains its shape and is composed of a band of pure ABA followed by a mixed band of ABA and Ile. As the concentration of the displacer is reduced, the composition of the isotachic azeotropic mixture varies along the unit selectivity line. Since this line crosses the C_B-axis, it is apparent that below a certain displacer concentration a pure band of B will also be obtained, since selectivity reversal is avoided. This is shown in Figure 6 which gives the calculated composition of the azeotropic mixture as a function of the displacer concentration. Only at displacer concentrations below approximately 30 mM is condition 1 satisfied, allowing a complete separation of the two components. This concentration value is, of course, not directly related to the point of occurrence of a crossing in the pure component isotherms, but is determined by the multicomponent uptake behavior.

Experimental displacement separations

Figure 7 shows displacement chromatograms obtained with a displacer concentration of 100 mM. Superimposed in this figure are the results of three separate runs in which the same feed loading was realized, but with different feed concentrations and column length. The time is in each case measured from the start of the displacer solution. The differences among the three experiments are only marginal, indicating that essentially the same constant state was attained in the experiments irrespective of the length traveled by the band and the initial width of the band. The salient feature of these results is that

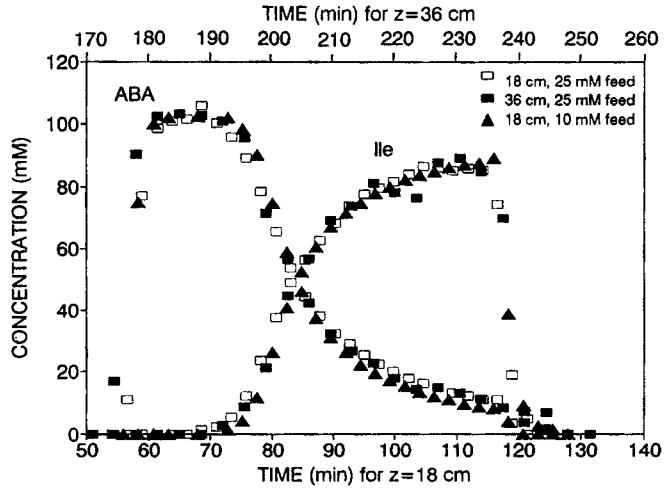

Figure 7. Displacement chromatography of equimolar ABA/Ile mixtures with Dowex 50W-X8.

[NaOH] = 100 mM, t_{load} = 120 min for 25 mM feed, t_{load} = 300 min for 10 mM feed.

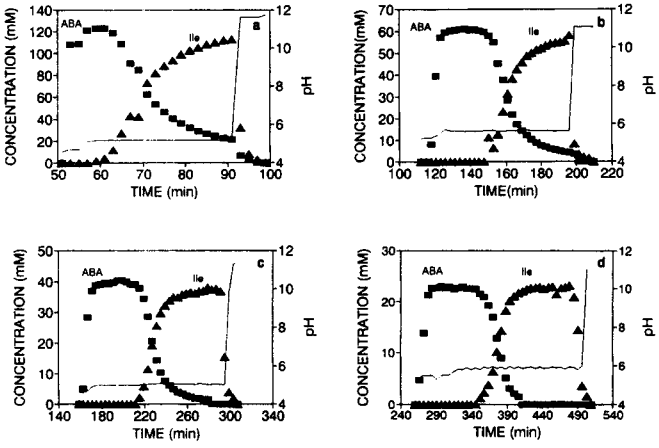

Figure 8. Displacement chromatography of 25 mM equimolar ABA/Ile mixtures with Dowex 50W-X8 for different displacer concentrations.

t_{load} = 100 min, z = 18 cm. (a) [NaOH] = 125 mM; (b) 60 mM; (c) 40 mM; (d) 25 mM.

only ABA, the early eluting species, is recovered in a pure form. Isoleucine, on the other hand, is eluted in a mixture with ABA. Moreover, the maximum effluent concentration of isoleucine is considerably lower than the isotachic value predicted by the Glueckauf condition, while the maximum concentration of ABA is very close to it. Because the column has a finite efficiency, the sharp bands predicted by the local equilibrium model are not observed and a "steady state" is reached instead. However, the formation of an azeotropic mixture in the development train is apparent as predicted from the uptake equilibrium behavior.

The results of a series of displacement chromatography experiments, performed with identical feed loading and column length but with a decreasing displacer concentration, is shown in Figure 8a-8d. A nearly pure band of α-ABA is obtained in all cases. Isoleucine, on the other hand, is recovered in a mixed band at high displacer concentrations. The isoleucine purity of this band gradually increases as the displacer concentration is reduced, until, at 25 mM NaOH, essentially pure isoleucine is recovered. Although the experimental results are not shown, we found that for these conditions, a constant state corresponding to a complete separation was attained independent of the initial bandwidth. The observed trends are again qualitatively consistent with the results of the local equilibrium analysis, although dispersed, rather than shock, transitions are obtained as a result of the finite efficiency of the resin column.

Numerical simulation

In order to simulate the experimental behavior, we used a numerical approximation of the conservation equations for the bed. To simplify the numerical calculations, we neglected the rates of accumulation of solutes in the interstitial liquid space. Since the resin capacity is quite high, the error resulting from this approximation is less than 10% in the prediction of the breakthrough time for the displacer front. The first term in Eq. 10, thus, could be discarded. The partial differential equations were then discretized by backward finite differences, following the procedure of DeCarli et al. (1990). After minor rearrangement, Eq. 10 yields:

$$\frac{dq_i^k}{dt} = \frac{u}{\rho_b \Delta z}\left(C_i^{k-1} - C_i^k\right) \tag{19}$$

The procedure is equivalent to modeling the bed with a series of N_s equilibrium stages. The resulting "numerical dispersion" introduces an approximate representation of physical dispersive effects such as hydrodynamic dispersion and mass-transfer resistances, as shown for example, by Lin et al. (1989).

Each displacement simulation consists of two stages: feed loading and displacement. During feed loading, integration of Eq. 19 over one time step is straightforward. Given the current values of C_i^k and C_i^{k-1}, incremented values of q_i^k are easily calculated for each stage from Eq. 19. With these incremented values of q_i^k, new C_i^k values are computed from the uptake equilibrium model. This is done by first computing the ionic fractions X_i in solution and obtaining the C_i^k values that satisfy the electroneutrality condition, as shown by Dinerman (1993). The integration is then continued with these new values. Simulation of displacement with this approach is, however, inefficient since an extremely sharp NaOH front is obtained. The amino acids become completely displaced by the high pH front and numerical instabilities and oscillations occur. In order to avoid cumbersome calculations, we simplified the integration by assuming that the displacer front is infinitely sharp and travels at the rate predicted by the local equilibrium model. Within the framework of the stage model, after a period of time $t_D = \Delta z / v_D$ elapsed from introduction of the displacer, the first stage in the column becomes fully saturated and the displacer begins to enter the second stage. During this period all of the feed components initially present in the first stage are removed. If we assume that the effluent concentrations from the first stage, C_i^1, remain constant for $0 < t < t_D$, we find:

$$C_i^1 = \frac{(q_i^1)^0}{q_0} C_D \tag{20}$$

where $(q_i^1)^0$ is the sorbent loading with species i when the displacer is first introduced to this stage. During the time $0 < t < t_D$ integration of the conservation equations for the remaining $N_s - 1$ stages continues in the same manner used during the feed loading step. At time $t = t_D$, the first stage is dropped, and the second stage is assumed to receive the displacer, while the conservation equations are integrated for the next $N_s - 2$ stages. The numerical process is continued until all N_s stages are eliminated and displacer breakthrough occurs. The method is, of course, not exact and the results would fail to predict any dispersion of the displacer front. On the other hand, if the number of stages is large, these results can be expected to provide a close approximation of ideal calculations describing the separation of the two feed components. A value of $N_s = 100$ was used since this value appeared to provide an adequate fit of the experimental data.

A comparison of the numerical solution with the experimental profiles obtained for the highest and lowest NaOH concentrations used experimentally is shown in Figure 9a and 9b. For a clearer comparison, the simulated profiles were shifted in time to match the experimental NaOH breakthrough point

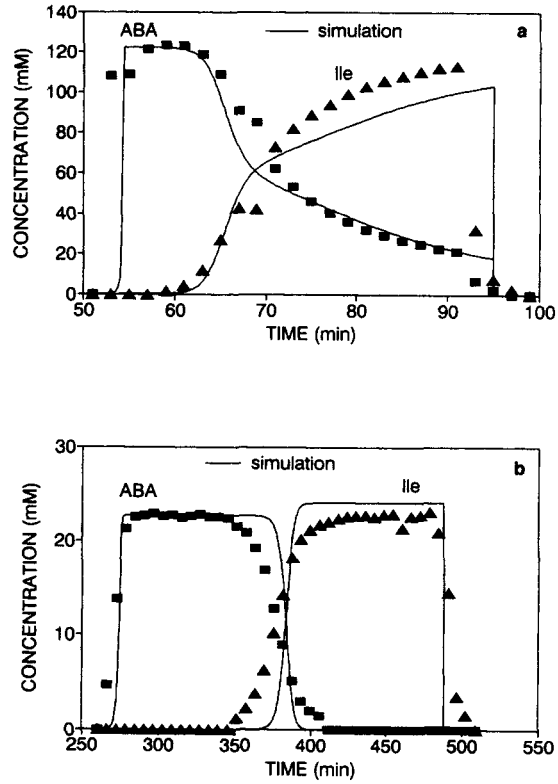

Figure 9. Comparison of experimental and simulated displacement separation of 25 mM equimolar ABA/Ile mixtures with Dowex 50W-X8.

t_{load} = 100 min, z = 18 cm. (a) [NaOH] = 125 mM; (b) 25 mM.

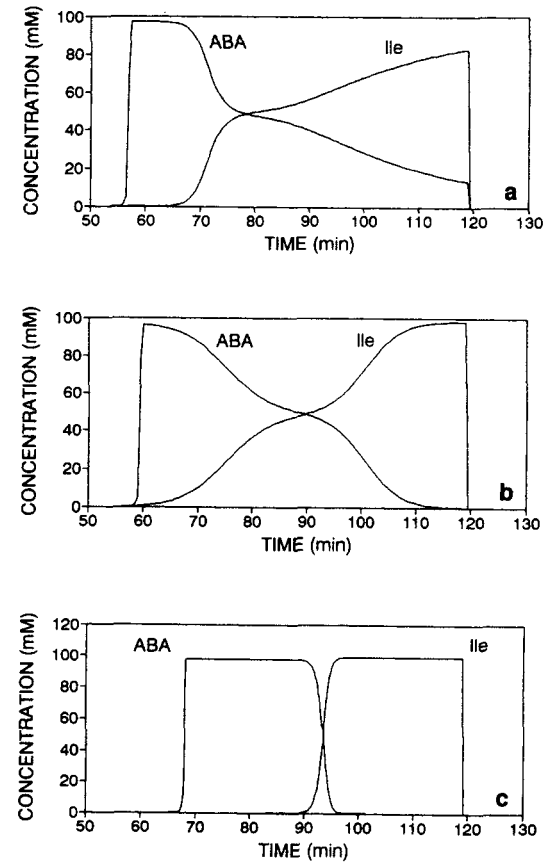

Figure 10. Comparison of simulated displacement separation for equimolar ABA/Ile mixtures for [NaOH] = 100 mM, t_{load} = 100 min, z = 18 cm.

(a) variable selectivity; (b) constant selectivity $\alpha_{B,A} = 1.28$; (c) constant selectivity $\alpha_{B,A} = 2.43$.

signaled by the sharp rise in pH. Such an adjustment compensated for having neglected the fluid phase accumulation term in Eq. 10, without affecting the shape of the profiles. For 125 mM NaOH the model predicts a sharp leading front for ABA, which is eluted in a very pure band. The isoleucine concentration is well predicted initially, but then significantly underestimated. The diffuse tail of α-ABA is, however, accurately predicted. These discrepancies arise in part because of the inability of the simple stage model to describe with great accuracy dispersive effects for nonlinear adsorption conditions and in part because of inaccuracies in the equilibrium uptake model. On the other hand, the numerical approximation captures the essential traits of the observed experimental behavior; namely, the appearance of a diffuse constant pattern with a pure leading component and a mixed late eluting mixture. Moreover, the numerical approximation correctly predicts a nearly complete separation when the displacer concentration is lowered to 25 mM (Figure 9b) as could have been concluded directly from the local equilibrium analysis.

The effects of the variation in the apparent selectivity are further highlighted in Figure 10. In this figure we compare numerical simulations of the displacement chromatography of the ABA/Ile mixture for a displacer concentration of 100 mM NaOH for three cases corresponding to the experimental system with variable selectivity; a case where the selectivity is a constant equal to the average selectivity coefficient ($\alpha_{B,A} = \bar{S}_{B,H}/\bar{S}_{A,H} = 1.28$); and a case where the selectivity coefficient is a constant equal to that each pure component has at infinite dilution ($\alpha_{B,A} = S^0_{B,H}/S^0_{A,H} = 2.43$). When $\alpha = 1.28$, the separation is still incomplete given the column length used for the simulations, but a pure band of isoleucine is obtained. Conversely, when the S-values at infinite dilution for each component are used, a complete separation is predicted. The latter two cases could of course only be attained in practice by changing the sorbent. To verify this possibility we carried out some runs with Dowex 50W-X4. This resin has the same dry weight capacity as the sample of Dowex 50W-X8 used. However, it has a much more open structure as a result of the much lower degree of cross-linking. Experimental profiles for the displacement chromatography of the two-component mixture are shown in Figure 11. Since the wet resin capacity is about 40% less than that of Dowex 50W-X8, the feed loading was also reduced by 40% for a direct comparison with the results in Figure 7. The important result is that now for 100 mM NaOH a complete separation is obtained. Selectivity reversal did not likely occur for these concentrations and is not apparent in the displacement profiles. This result is consistent with the observations of Jones and Carta (1993) that essentially ideal equilibrium behavior is seen for resins with a degree of cross-linking less than about 6%. A drawback of using such resins is, of course, that the resin capacity per unit volume is reduced significantly relative to the previous case. Both components

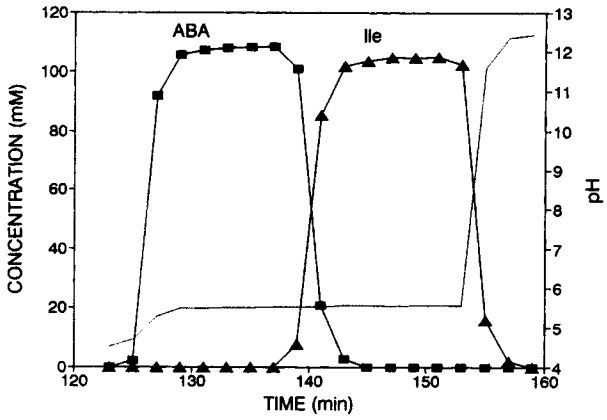

Figure 11. Displacement chromatography of a 25 mM equimolar ABA/Ile mixture with Dowex 50W-X4.

[NaOH] = 100 mM, t_{load} = 60 min, z = 36 cm.

are however recovered in pure form at a high concentration, approximately equal to the displacer concentration.

In closing, it is of interest to consider the predicted behavior when the feed mixture is located in the hodograph plane to the left of the unit selectivity line. This situation was not investigated experimentally, but is exemplified through numerical simulations in Figure 12. The simulations were performed with $N_s = 100$ with a displacer concentration of 100 mM, and with a feed mixture containing 5 mM ABA and 80 mM Ile. In the first case, Figure 12a, the simulation was performed for the equilibrium parameter values corresponding to the experimental system with Dowex 50W-X8. A small pure band of Ile is formed at the leading front of the displacement train,

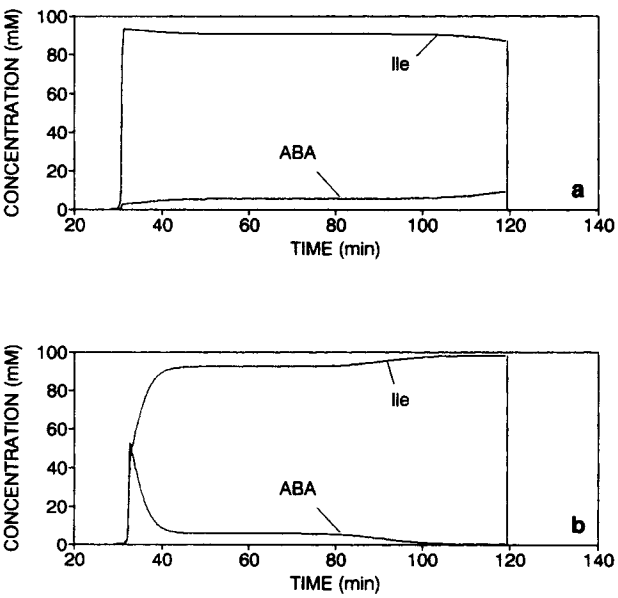

Figure 12. Comparison of simulated displacement separation for a ABA/Ile mixture with $C_A = 5$ mM and $C_B = 80$ mM for [NaOH] = 100 mM, $t_{load} = 100$ min, $z = 18$ cm.

(a) variable selectivity; (b) constant selectivity $\alpha_{B,A} = 1.28$.

with a slight "roll-up" of Ile above the feed concentration. At the rear boundary of the profiles, ABA and Ile co-elute as a mixed band. Under ideal conditions (that is, for $N_s \to \infty$), the composition of this band would be located on the unit selectivity line in the hodograph plane. In the second case, Figure 12b, the simulation was performed for constant selectivity values, $\alpha_{B,A} = 1.28$, for otherwise identical conditions. Since selectivity reversal does not occur in this case, the classical development of bands with an intermediate plateau is seen. The leading boundary contains a concentrated portion of ABA (complete purity is not achieved here because of the small number of stages), while the rear boundary consists of a pure band of the more strongly preferred component, Ile.

Conclusions

We have reported data on an experimental two-component ion-exchange system which appears to exhibit a reversal of the selectivity coefficient as the ionic composition is varied. This reversal is manifested in an incomplete separation of a binary mixture in displacement chromatography, with only the early eluting species recovered in a pure band. For the system investigated, the formation of azeotropic mixtures during the development of concentration bands is dependent upon the displacer concentration. At low concentrations, the resin loading with solutes is sufficiently low that the equilibrium is nearly ideal. For these conditions, a complete separation of the two species is obtained. At high concentrations, however, the resin becomes almost completely saturated and nonideal equilibrium effects leading to an incomplete separation are evident.

An analogy to azeotropes found in constant-pressure batch distillation can be drawn, as suggested, for example, by Antia and Horvath (1991). Although for a given pressure a single azeotropic composition may be obtained in a binary distillation, different azeotropes may be reached if the pressure is varied. Similarly, in displacement chromatography of a binary mixture, azeotropic bands of different composition may be obtained depending upon the displacer concentration. For the case investigated, these azeotropic band compositions lie on a single unit-selectivity line in the hodograph plane. In general, as in distillation, the occurrence or breakdown of azeotropic mixtures is dependent upon the nature of the multicomponent phase equilibrium that governs the separation, and different types of azeotropic behavior are observed in adsorption systems, as shown by Basmadjian et al. and Antia and Horvath.

The equilibrium uptake model used in the analysis of the experimental results for the ABA/Ile separation provides an excellent representation of the single component uptake behavior. The same model can be used to make predictions of multicomponent equilibria. Such predictions, although only approximate, appear to be quite consistent with the anomalous development of component bands in displacement chromatography. In particular, we found that the model could be conveniently used to determine what displacer concentration could be used to yield essentially pure component bands.

Notation

C_i = concentration of species i in solution, mmol/L
C_i^k = concentration of species i for state k, mmol/L
C_i^* = concentration of species i obtained from Glueckauf relationship (Eq. 2), mmol/L

K_1 = dissociation constant for protonated amino acid, mol/L
K_2 = dissociation constant for zwitterionic amino acid, mol/L
K_W = ionic product of water, $(mol/L)^2$
N = number of counterions
N_s = number of stages
q_i = concentration of species i in resin, mmol/g dry resin
q_0 = resin ion-exchange capacity, meq/g dry resin
$S_{i,j}$ = selectivity coefficient for exchange of species i and j
$S^0_{i,j}$ = selectivity coefficient for exchange of species i and j at infinite dilution
$\bar{S}_{i,j}$ = equilibrium parameter for exchange of ions i and j
t = time, s
t_D = time to saturate one stage with displacer, s
t_{load} = duration of feed loading, s
u = superficial velocity, cm/s
v = interstitial velocity, cm/s
v_D = velocity of displacer front, cm/s
v_i = concentration velocity of species i, cm/s
v_i^s = shock velocity of species i, cm/s
$W_{i,j}$ = equilibrium parameter for exchange of ions i and j
X_i = ionic fraction of cationic species i in solution
Y_i = ionic fraction of species i in resin
z = column axial coordinate or length, cm

Greek letters

$\alpha_{i,j}$ = separation factor for species i and j
ϵ = bed void fraction
ρ_b = bed density, g dry resin/cm^3 bed

Literature Cited

Antia, F. D., and Cs. Horvath, "Analysis of Isotachic Patterns in Displacement Chromatography," *J. Chromatog.*, **556**, 119 (1991).

Basmadjian, D., P. Coroyannis, and C. Karayannopoulos, "Equilibrium Theory Revisited. Isothermal Fixed-Bed Sorption of Binary Systems: II. Non-Langmuir Solutes with Type I Parent Isotherms: Azeotropic Systems," *Chem. Eng. Sci.*, **42**, 1737 (1987).

Carta, G., M. S. Saunders, J. P. DeCarli, II, and J. B. Vierow, "Dynamics of Fixed-Bed Separations of Amino Acids by Ion Exchange," *AIChE Symp. Ser.*, **84**, 54 (1988).

Cramer, S. M., "Novel Displacement Chromatographic Systems for Protein Purification from Complex Biological Mixtures," Int. Symp. on Preparative Chromatography, Arlington, VA (1993).

de Bokx, P. K., P. C. Baarslag, and H. P. Urbach, "Modeling of Displacement Chromatography using Non-Ideal Isotherms," *J. Chromatog.*, **594**, 9 (1992).

DeCarli, J. P., II, G. Carta, and C. H. Byers, "Displacement Separations by Continuous Annular Chromatography," *AIChE J.*, **36**, 1220 (1990).

Dinerman, A. A., "Displacement Chromatography of Amino Acids: Equilibrium and Selectivity Reversal Effects," MS Thesis, Univ. of Virginia, Charlottesville (1993).

Dye, S. R., J. P. DeCarli, II, and G. Carta, "Equilibrium Sorption of Amino Acids by a Cation Exchange Resin," *Ind. Eng. Chem. Res.*, **29**, 849 (1990).

Glueckauf, E., "Theory of Chromatography: VII. General Theory of Two Solutes Following Nonlinear Isotherms," *Discuss. Farad. Soc.*, **7**, 12 (1949).

Gosling, I. S., D. Cook, and M. D. M. Fry, "The Role of Adsorption Isotherms in the Design of Chromatographic Separations for Downstream Processing," *Chem. Eng. Res. Dev.*, **67**, 232 (1989).

Helfferich, F., *Ion Exchange*, McGraw-Hill, New York, p. 151 (1962).

Helfferich, F., and G. Klein, *Multicomponent Chromatography*, Marcel Dekker, New York (1970).

Jones, I. L., and G. Carta, "Ion Exchange of Amino Acids and Dipeptides on Cation Resins with Varying Degree of Crosslinking: I. Equilibrium," *Ind. Eng. Chem. Res.* **32**, 107 (1993).

Kemball, C., E. K. Rideal, and E. A. Guggenheim, "Thermodynamics of Monolayers," *Trans. Farad. Soc.*, **44**, 948 (1948).

Lin, B., Z. Ma., and G. Guiochon, "Influence of Calculation Errors in the Numerical Simulation of Chromatographic Elution Band Profiles using an Ideal or Semiideal Model," *J. Chromatog.*, **484**, 83 (1989).

Meister, A., *Biochemistry of the Amino Acids*, Vol. I, Academic Press, New York (1965).

Myers, A. L., and J. M. Prausnitz, "Thermodynamics of Mixed Gas Adsorption," *AIChE J.*, **11**, 121 (1965).

Myers, A. L., and S. Byington, "Thermodynamics of Ion Exchange: Prediction of Multicomponent Equilibria from Binary Data," *Ion Exchange Science and Technology*, A. E. Rodrigues, ed., NATO ASI Ser. E, No. 107, Nijhoff, Dordrecht, The Netherlands, p. 119 (1986).

Paludetto, R., G. Gamba, G. Storti, S. Carra', and M. Morbidelli, "Multicomponent Adsorption Equilibrium of Highly Non-Ideal Mixtures: the Case of Chloroaromatic Mixtures on Zeolites," *Chem. Eng. Sci.*, **42**, 2713 (1987).

Partridge, S. M., and R. C. Brimley, "Displacement Chromatography on Synthetic Ion-Exchange Resins: 8. A Systematic Method for the Separation of Amino Acids," *Biochem.*, **51**, 628 (1952).

Rhee, H.-K., and N. R. Amundson, "Analysis of Multicomponent Separation by Displacement Development," *AIChE J.*, **28**, 423 (1982).

Ruthven, D. M., *Principles of Adsorption and Adsorption Processes*, Wiley, New York, p. 279 (1984).

Saunders, M. S., J. B. Vierow, and G. Carta, "Uptake of Phenylalanine and Tyrosine by a Strong-Acid Cation Exchanger," *AIChE J.*, **35**, 53 (1989).

Subramanian, G., and S. M. Cramer, "Displacement Chromatography of Proteins Under Elevated Flow Rate and Crossing Isotherm Conditions," *Biotechnol. Prog.*, **5**, 92 (1989).

Yu, Q., J. Yang, and N.-H. L. Wang, "Multicomponent Ion Exchange Chromatography for Separating Amino Acid Mixtures," *React. Poly.*, **6**, 33 (1987).

Manuscript received Aug. 2, 1993, and revision received Nov. 4, 1993.